JOURNAL GEOLOGICAL SOCIETY OF INDIA
Vol.92, October 2018, pp.449-456

Assessment of Vulnerability of Rock Slope Considering Material and Seismic Variability

Nishant Roy[1], Rajib Sarkar[2*], Kripamoy Sarkar[3], Mahesh Kumar Jat[1] and Gaurav Fulwaria[1]

[1]Department of Civil Engineering, MNIT Jaipur- 302 017, India
[2]Department of Civil Engineering, [3]Department of Applied Geology, IIT (ISM) Dhanbad - 826 004, India
E-mail: *nishantciv@gmail.com; rajibdeq@gmail.com*; kripamoy.sarkar@gmail.com; mahesh.mnit@gmail.com; gk.churu@gmail.com*

ABSTRACT

Stability analysis of rock slopes has always been a critical and challenging task for the geotechnical engineering professionals. The complexities associated with the stability analysis arise due to the heterogeneous, anisotropic and variable nature of the rock mass. Assessment of slope stability becomes further challenging under earthquake motions which are random in nature. Thus, uncertainties in both material and loading parameters are required to be considered for a robust assessment of the vulnerability of slopes in geologically complex and seismically active regions.

In the present study, the influence of variability in geological properties on the slope stability has been considered within the framework of First Order Reliability Method (FORM). Reliability analysis has been performed for a typical slope profile using the Response Surface Method (RSM) and FORM leading to the identification of critical design parameters along with the quantification of the system performance in terms of reliability index. Subsequently, dynamic time history analyses have been performed for generating the seismic fragility curves of the rock slope as a function of increasing earthquake intensity. Thus, the study attempts to present a methodology for assessing the vulnerability of a rock slope with due consideration of the variation in both the material properties and seismic loading.

INTRODUCTION

The assessment of the performance of slopes is a major field in geotechnical engineering associated with uncertainties arising due to the variable nature of the geological medium. Properties of rock mass characterized in terms of strength and deformation parameters such as cohesion (c), friction angle (ϕ), elastic modulus (E) and unit weight (γ) is known to be associated with wide spatial variation (Phoon and Kulhawy 1999). For an adequate assessment of slope performance, a due consideration of the associated uncertainties becomes crucial. Reliability methods constitute a robust class of probabilistic approach which allows systematic consideration of the uncertainties in the evaluation of system performance (Li and Low 2010, Low and Einstein 2013). Such approaches overcome the limitations of conventional deterministic methods, providing better flexibility to engineers to evaluate system performance. Among various methods, the First Order Reliability Method (FORM) has emerged as a popular method for the evaluation of performance of a number of geotechnical systems (Xu and Low 2006, Low and Tang 1997, Low and Tang 2007, Li and Low 2010, Lu and Low 2011, Low and Einstein 2013). This method has also been extensively applied in the probabilistic assessment of slope performance.

Another form of uncertainty associated with the evaluation of performance of slopes is due to the variable seismic motion which may act in tectonically active regions. Since these slopes serve as lifeline facilities in mountainous regions, evaluation of seismic performance assumes great significance. One of the effective ways of evaluating the performance of slope under variable seismic conditions is through the use of seismic fragility curves (Rossetto and Elnashai 2003, Pitilakis et al. 2014). These curves relate the probability of unsatisfactory performance of any infrastructural facility with increasing intensity of earthquake motions (Andersen et al. 2008).

For effective planning of lifeline facilities in mountainous regions, a due consideration of both the forms of uncertainties, i.e., variable geological and seismic settings, needs to be considered. However, till date, these two approaches have been rarely utilized concurrently. The present study attempts to employ these two approaches for assessing the performance of a rock slope incorporating both the material and seismic variability. Such an approach facilitates the assessment of the seismic vulnerability of a given slope in a robust manner.

The highlights of the present study are:

- Influence of uncertainty of material parameters on the stability of a typical rock slope, has been examined using the Response Surface Method (RSM) and First Order Reliability Method (FORM).
- The most critical combination of variable parameters, i.e., critical design parameters have been evaluated. The critical combination has been subsequently utilized in the dynamic finite element analyses of the slope for assessment of various performance levels of the rock slope.
- The influence of seismic motion on the slope performance have been evaluated through the generation of the seismic fragility curves which comprehensively take into account the effect of both the frequency and amplitude of the dynamic waves.

METHODOLOGY

The methodology adopted in the present study attempts to incorporate the geological and seismic variability by coupling the First Order Reliability Method (FORM) followed by the derivation of seismic fragility curves. The results obtained from the FORM and expressed in terms of critical design points represent the combination of random parameters likely to cause the worst performance of the slope under pseudo-static conditions. Adopting these design points, the effect of dynamic nature of earthquake time histories on the performance of the slope is evaluated through the generation of seismic fragility curves. In the following sections, a brief description of the methodology along with their application for the considered slope has been discussed.

FORM and Hasofer-Lind Reliability Index

Reliability methods provide a robust and rational approach to efficiently take into consideration the inherent uncertainties associated

0016-7622/2018-92-4-449/$ 1.00 © GEOL. SOC. INDIA | DOI: 10.1007/s12594-018-1040-5

with any engineering system. Many different reliability methods have evolved over the years which have found wide application in the field of geotechnical engineering. Among various methods, the FORM has emerged as a popular method for assessing the system performance through the evaluation of reliability index.

A popular reliability method based on FORM, which has been utilized in the present study, is the 'Hasofer-Lind' method (Hasofer and Lind 1974, Low and Tang 2007). In this method, the assessment of the reliability index is mainly based on the reduction of the problem to a standardized coordinate system. Thus, a random variable X_i is reduced as per Eqn (1).

$$X_i' (X_i - \mu_{x_i})/\sigma_{x_i} \qquad (i = 1,2,3, ..., n) \qquad (1)$$

where X_i' is a random variable with zero mean and unit standard deviation. X denotes the random variable in original coordinate system and X' denotes random variable in reduced coordinate system. In reduced system, the Hasofer-Lind reliability index β_{HL} is the minimum distance from the origin of the axes to the limit state surface and may be evaluated using Eqn (2),

$$\beta_{HL} = \sqrt{(X'^{*})^{T} * (X'^{*})} \qquad (2)$$

where X'^{*} is the vector of the design points in the reduced coordinate system.

An alternative interpretation of the Hasofer-Lind reliability index evaluated using FORM, has been discussed by Low and Tang (1997, 2007). The description is based on the concept of an expanding ellipsoid and is mathematically expressed in terms of Eq. (3) and (4).

$$\beta = \min_{x \in F} \sqrt{(x-\mu)^{T} C^{-1} (x-\mu)} \qquad (3)$$

$$\beta = \min_{x \in F} \sqrt{\left[\frac{x_i - \mu_i}{\sigma_i}\right]^{T} R^{-1} \left[\frac{x_i - \mu_i}{\sigma_i}\right]} \qquad (4)$$

where x represents the vector of set of random variables x_i, μ is the vector of set of mean values μ_i, C is the covariance matrix, R is the correlation matrix, σ_i is the standard deviation and F is the failure domain. The procedure for computing the reliability index β is to transform the failure surface into the space of reduced variable. Shortest distance from the transformed failure surface to the origin of the reduced variables gives the reliability index.

As suggested by Low and Tang (2007), the concept of expanding ellipse presented in Fig. 1 leads to a simple method for computing the Hasofer-Lind reliability index. In terms of an expanding ellipsoid, the sample points x_i of random variables which minimizes Eq. (4) and belong to the failure domain *i.e.* $x \in F$, represents the design point. They are also known as the most probable point of failure and correspond to an expanding ellipsoid which is tangential to the limit state surface demarcating the domain between safe and unsafe regions as shown in Fig. 1.

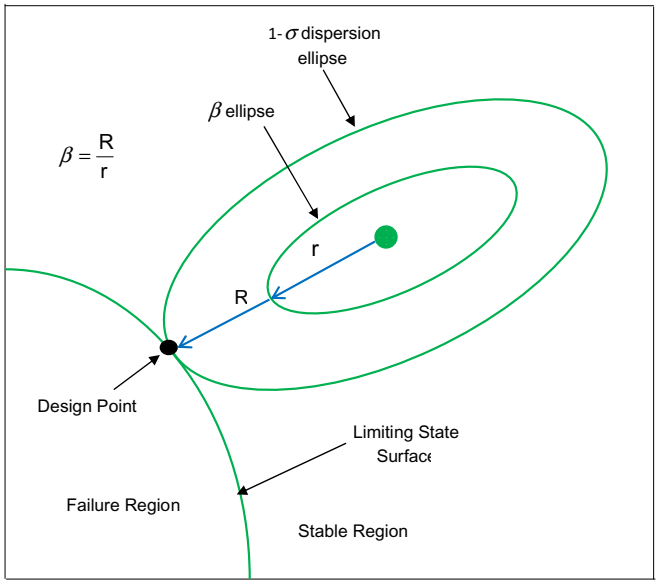

Fig.1. Hasofer Lind reliability index and design point expressed in terms of expanding dispersion ellipsoid (after Low and Tang, 2007).

Response Surface Method

To carry out reliability analysis using FORM, explicit formulation of performance function is required. However, in case of complicated and non-linear systems where the system response is evaluated using numerical analyses, explicit representation of the performance function in terms of random variables may be very difficult. In such cases, Response Surface Method (RSM) is utilized to frame the performance function.

The RSM has been extensively used in a number of civil engineering problems (Mollon et al. 2009, Bucher and Bourgund, 1990, Rajashekhar and Ellingwood, 1993, Tandjiria et al. 2000, Chan and Low, 2009). The fundamental concept of the RSM approach depends on the construction of a closed form polynomial equation g'(X), known as the response surface, based on limited number of deterministic analyses. This mathematical equation relating the system response with the input parameters is then utilized to approximate the critical limit state surface at the point nearest to the set of mean parameters thereby providing an assessment of the reliability index. Thus RSM may be viewed as a powerful tool providing a bridge between the existing deterministic methods and the reliability methods (Lu and Low 2011).

CRITICAL DESIGN POINTS OF A ROCK SLOPE BY FORM

Numerical Model of the Rock Slope

It may be stated that the choice between two-dimensional and three-dimensional numerical modelling approaches for assessment of slope stability is dependent on curvature effect. Hoek (1970) and Hoek and Bray (1977) summarised that three-dimensional model needs to be adopted in case slopes are either concave or convex. Thus, if the lateral curvature (curvature in the plan) of the slope is prominent, three-dimensional model proves to be more appropriate. However, in case of the slope being long and straight in lateral direction, the two-dimensional model seems to be a suitable choice considering the additional computational burden in case of three-dimensional model. Moreover, the factor of safety evaluated using two-dimensional analysis is generally more conservative in comparison to three-dimensional analysis (Cavounidio 1987). Considering the ensuing discussion, it has been considered that the slope is long and straight and hence two-dimensional modeling is assumed to be appropriate. However, the procedure highlighted in the present study may be extended to the three-dimensional case.

A schematic representation of the slope considered in the present study is shown in Fig. 2. The slope has a fixed height (H) of 50 m with variable slope angle (β). In order to minimize the effect of artificial boundaries, the model dimensions have been finalized as per the recommendations of Wyllie and Mah (2004). Bottom boundary of the model has been fixed in all directions whereas the lateral boundaries have been restrained in the horizontal direction. Mohr-Coulomb constitutive law has been considered for the rock mass. The number of elements used in each model has been decided based on mesh sensitivity analyses. The assessment of slope stability has been achieved through the use of Strength Strength Reduction (SSR) technique as incorporated in the finite element package. A discretized view of finite element model of the slope is shown in Fig.3.

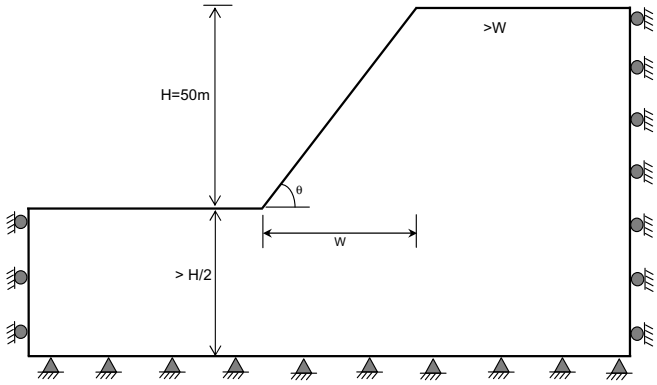

Fig.2. A schematic representation of numerical model.

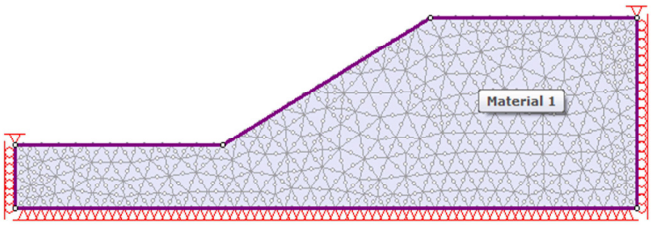

Fig.3. Finite element model showing discretized slope.

Random Parameters Considered in the Study

To quantify the stability of the rock slope, the widely used Shear Strength Reduction (SSR) technique has been applied on the numerical model using finite element based software RS2.0 (Rocscience Inc. 2015). The SSR technique leads to the evaluation of the Strength Reduction Factor (SRF) (Zienkiewicz et al., 1975, Donald and Giam, 1988, Matsui and San, 1992, Ugai and Leshchinsky,1995, Dawson et al., 1999, Griffiths and Lane, 1999, Cheng et al., 2007, Wei et al., 2009, Cai and Ugai, 2000, Won et al., 2005, Wei and Cheng, 2009, Griffiths et al., 2010, Yang et al., 2011, Rathod and Rao, 2012, Zhang et al., 2015). A value of SRF less than 1 corresponds to the case of instability. The parameters affecting the strength behavior of the geological medium and the loading conditions have a significant influence on the value of the computed SRF. Moreover, the deformation of the slope is also an important criterion governing the serviceability of the slope providing a useful insight of the regions along the slope which may be prone to instabilities.

However, the parameters characterizing the strength and deformation behavior of the rock mass and the loading conditions may not have a specific value at a given site due to the inherent variability associated with geology and the tectonic setting. Hence a due consideration of the variability in stability assessment assumes significance. To account for the variability, a total of five random variables have been considered which have been mentioned below for brevity.

1. Cohesion of the rock mass, c
2. Friction angle of the rock mass, ϕ
3. Young's modulus of rock mass, E
4. Slope angle, θ
5. Pseudo-static coefficient of horizontal acceleration, k_h

The choice of type of statistical distribution for random parameters has been made based on the suggestions made in a number of studies and engineering judgment. Normal and truncated normal distribution has been suggested for the friction angle of the geological medium in the literature (Mostyn and Li 1993, Nilsen 2000, Pathak and Nilsen 2004). Cohesion is also reported to follow a normal distribution (Song et al., 2011). The pseudo-static horizontal coefficient and Young's modulus are also assumed to follow a normal distribution whereas linear distribution has been adopted for slope angle. Table 1 presents the mean, coefficient of variation and standard deviation of the random variables considered for the present analyses. The unit weight of the rock mass is considered to be 18.50 kN/m^3 (Shen et al., 2014).

Table 1. Random variables considered in the present study

Parameters	Distribution	Mean	COV (%)	Std. Dev.
c (MPa)	Normal	0.2	40	0.08
ϕ (Degree)	Normal	30	20	6.00
E (MPa)	Normal	1200	40	480
θ (Degree)	Linear	45	-	8.66
k_h	Normal	0.15	-	0.10

Performance Function and Reliability Index

In the present study, the stability of the slope has been evaluated by utilizing the Shear Strength Reduction (SSR) technique which expresses the results in terms of Strength Reduction Factor (SRF). Based on the values of the SRF evaluated through deterministic numerical simulations, the performance function has been framed for reliability analysis of the slope.

Framing the Performance Function

In the present study, a total of 32 number of deterministic analyses (2^n simulations where n is number of random parameters) have been carried out in each iteration. Table 2 presents the SRF values computed for various combinations of input parameters for various combinations of input parameters. Based on the SRF values

Table 2. SRF from pseudo-static analysis for first iteration

Sl. No.	c (MPa)	ϕ (Degree)	E (MPa)	θ (Degree)	k_h	SRF
1	0.28	36	720	30	0.05	3.66
2	0.28	36	1680	30	0.05	3.66
3	0.28	24	720	30	0.05	2.95
4	0.28	24	1680	30	0.05	2.95
5	0.12	36	720	30	0.05	2.49
6	0.12	36	1680	30	0.05	2.49
7	0.12	24	720	30	0.05	1.87
8	0.12	24	1680	30	0.05	1.87
9	0.12	36	1680	30	0.25	1.73
10	0.12	36	720	30	0.25	1.73
11	0.28	24	720	30	0.25	2.00
12	0.28	36	1680	30	0.25	2.52
13	0.28	36	720	30	0.25	2.52
14	0.28	24	1680	30	0.25	2.00
15	0.12	24	1680	30	0.25	1.30
16	0.12	24	720	30	0.25	1.30
17	0.12	24	720	60	0.25	0.86
18	0.12	36	720	60	0.25	1.08
19	0.12	24	1680	60	0.25	0.86
20	0.28	24	720	60	0.25	1.46
21	0.28	36	720	60	0.25	1.74
22	0.28	36	1680	60	0.25	1.74
23	0.28	24	1680	60	0.25	1.46
24	0.12	36	1680	60	0.25	1.08
25	0.28	24	1680	60	0.05	1.95
26	0.28	24	720	60	0.05	1.95
27	0.12	36	720	60	0.05	1.44
28	0.12	36	1680	60	0.05	1.44
29	0.12	24	1680	60	0.05	1.14
30	0.12	24	720	60	0.05	1.14
31	0.28	36	1680	60	0.05	2.31
32	0.28	36	720	60	0.05	2.31

computed in any iteration, a response surface $G(X)$ is derived. The performance function is formulated as per Eq. (5) which implies that the slope remains stable in case of SRF values greater than 1.

$$g'(X) = G(X) - 1 \quad (5)$$

Reliability Index of the Slope Configuration and Design Points

The reliability index is evaluated using a spreadsheet based optimization tool SOLVER in MS-EXCEL. Based on the performance function and the variations in input parameters, a reliability index β_1 of 1.77 is obtained in the first iteration. The values of random variables at design point for the first iteration are shown in Table 3. Using these design points, the center points are updated and the process is repeated to frame the new response surface and performance function. The details of the 32 number of deterministic analyses for the second iteration are presented in Table 4. The second iteration led to a reliability index β_2 of 1.89. The design points obtained in the second iteration are also shown in Table 3.

The details of various input parameters and the corresponding SRF values for the third iteration are presented in Table 5. The response surface generated using regression analyses for the third iteration is given by Eq. (6). The reliability index evaluated based on the performance function framed using Eq. (6) is 1.80. Thus, a convergence is obtained in the third iteration with the reliability index β_3 of 1.80.

$$(SRF)_3 = 0.95 + 4.37c + 0.02\phi - 0.009\theta - 2.09k_h \quad (6)$$

Thus, three iterations have been carried out in the present study to arrive at the design points which have been listed in Table 6. These design points correspond to the most critical combination of input parameters. It may be noted here that the pseudo-static analyses presented in the present section does not take into consideration the interaction between the dynamic waves and the slopes. Moreover, the SRF values correspond to the ultimate limit state with regard to system performance. It does not provide any insight with regard to the serviceability criterion. In order to account for the variability in dynamic loading characterized in terms of frequency and amplitude, dynamic time history analyses have been carried out with the material properties set equal to the design points identified at this stage. The subsequent section provides a detailed discussion with regard to the generation of the seismic fragility curves based on which the slope performance may be evaluated.

Table 3. Design points obtained in first two iterations

Iteration-1		Iteration-2	
Variables	Values	Variables	Values
c (MPa)	0.08	c (MPa)	0.07
ϕ (Degree)	26.99	ϕ (Degree)	25.79
θ (Degree)	48.37	θ (Degree)	48.28
k_h	0.18	k_h	0.18

Table 4. SRF from pseudo-static analysis for second iteration

Sl. No.	c (MPa)	ϕ (Degree)	E (MPa)	θ (Degree)	k_h	SRF
1	0.09	26.31	719.99	30	0.13	1.51
2	0.09	26.31	1679.99	30	0.13	1.51
3	0.09	14.31	719.99	30	0.13	1.04
4	0.09	14.31	1679.99	30	0.13	1.04
5	0.03	26.31	719.99	30	0.13	1.01
6	0.03	26.31	1679.99	30	0.13	1.01
7	0.03	14.31	719.99	30	0.13	0.76
8	0.03	14.31	1679.99	30	0.13	0.76
9	0.03	26.31	1679.99	30	0.25	0.82
10	0.03	26.31	719.99	30	0.25	0.82
11	0.09	14.31	719.99	30	0.25	0.84
12	0.09	26.31	1679.99	30	0.25	1.22
13	0.09	26.31	719.99	30	0.25	1.22
14	0.09	14.31	1679.99	30	0.25	0.84
15	0.03	14.31	1679.99	30	0.25	0.57
16	0.03	14.31	719.99	30	0.25	0.57
17	0.03	14.31	719.99	60	0.25	0.55
18	0.03	26.31	719.99	60	0.25	0.68
19	0.03	14.31	1679.99	60	0.25	0.55
20	0.09	14.31	719.99	60	0.25	0.67
21	0.09	26.31	719.99	60	0.25	0.76
22	0.09	26.31	1679.99	60	0.25	0.76
23	0.09	14.31	1679.99	60	0.25	0.67
24	0.03	26.31	1679.99	60	0.25	0.68
25	0.09	14.31	1679.99	60	0.13	0.81
26	0.089	14.31	719.99	60	0.13	0.81
27	0.025	26.31	719.99	60	0.13	0.92
28	0.025	26.31	1679.99	60	0.13	0.92
29	0.025	14.31	1679.99	60	0.13	0.74
30	0.025	14.31	719.99	60	0.13	0.74
31	0.09	26.31	1679.99	60	0.13	0.91
32	0.09	26.31	719.99	60	0.13	0.91

Table 5. SRF from pseudo-static analysis for third iteration

Sl. No.	c (MPa)	ϕ (Degree)	E (MPa)	θ (Degree)	k_h	SRF
1	0.13	24.65	719.99	30	0.14	1.7
2	0.13	24.65	1679.99	30	0.14	1.7
3	0.13	12.65	719.99	30	0.14	1.21
4	0.13	12.65	1679.99	30	0.14	1.21
5	0.01	24.65	719.99	30	0.14	0.75
6	0.01	24.65	1679.99	30	0.14	0.75
7	0.01	12.65	719.99	30	0.14	0.61
8	0.01	12.65	1679.99	30	0.14	0.59
9	0.01	24.65	1679.99	30	0.25	0.61
10	0.01	24.65	719.99	30	0.25	0.61
11	0.13	12.65	719.99	30	0.25	0.98
12	0.13	24.65	1679.99	30	0.25	1.39
13	0.13	24.65	719.99	30	0.25	1.39
14	0.13	12.65	1679.99	30	0.25	0.98
15	0.01	12.65	1679.99	30	0.25	0.44
16	0.01	12.65	719.99	30	0.25	0.44
17	0.01	12.65	719.99	60	0.25	0.28
18	0.01	24.65	719.99	60	0.25	0.32
19	0.01	12.65	1679.99	60	0.25	0.28
20	0.13	12.65	719.99	60	0.25	0.71
21	0.14	24.65	719.99	60	0.25	0.93
22	0.14	24.65	1679.99	60	0.25	0.93
23	0.13	12.65	1679.99	60	0.25	0.71
24	0.01	24.65	1679.99	60	0.25	0.33
25	0.13	12.65	1679.99	60	0.13	0.84
26	0.13	12.65	719.99	60	0.13	0.84
27	0.01	24.65	719.99	60	0.13	0.8
28	0.01	24.65	1679.99	60	0.13	0.78
29	0.01	12.65	1679.99	60	0.13	0.59
30	0.01	12.65	719.99	60	0.13	0.57
31	0.13	24.65	1679.99	60	0.13	1.09
32	0.13	24.65	719.99	60	0.13	1.09

Table 6. Critical design points obtained for the rock slope

Variables	Values
c (MPa)	0.07
ϕ (Degree)	26.68
E (MPa)	1200
θ (Degree)	48.04
k_h	0.18

GENERATION OF SEISMIC FRAGILITY CURVES

Overview of Seismic Fragility Curves

Seismic fragility curves provide a robust tool for probabilistic risk assessment of geotechnical systems (Rossetto and Elnashai, 2003, Argyroudis and Pitilakis, 2012, Argyroudis and Kaynia, 2015). The fragility curve relates the probability of unsatisfactory performance of any system with increasing intensity of earthquake motions. In a broad sense, the uncertainty associated with probable seismic scenarios is effectively considered in the assessment of the vulnerability of the system through these curves (Andersen et al., 2008). Thus, it provides a robust and flexible tool to designers in evaluating the relative performance based on various criteria with probable ground motion thereby striking a balance between safety and economy.

In the following sections, a brief description about the performance levels and methodology for the generation of fragility curves is discussed. Subsequently, the dynamic analyses of the slope considered in present study have been explained. This is followed by a discussion on the fragility curves generated for the slope.

Performance Levels

The assessment of seismic vulnerability or risk of a geotechnical structure may be defined in terms of damage thresholds known as limit states. A limit state represents the boundary between different performance levels. Thus, depending upon the nature and functionality of the geotechnical structure under consideration, one may adopt different limit states based on engineering judgment.

In case of mountainous slopes, the assessment of seismic vulnerability of the road element holds crucial importance as any loss in its functionality leads to adverse impact on the socio-economic activities of the region. Thus, any attempt to assess the seismic vulnerability must be reflective of the consequences arising from different performance levels.

A number of studies have been made for fragility assessment of slopes and roadway elements (NIBS 2004; Maruyama et al. 2010). In the aforementioned studies, different damage states have been considered depending on the functionality, state of traffic, duration and the cost involved in repair. The damage states primarily relate to the extent of settlement or offset of the ground, movement and/or cracking of the pavement. The intensity measure threshold adopted in these studies includes peak ground velocity (PGV), peak ground acceleration (PGA) and permanent ground displacement (PGD).

A detailed discussion on the damage index has been provided in European project SYNER-G considering roadway and railway elements (Kaynia et al. 2011). The same benchmark has also been utilized in studies dealing with generation of fragility curves for embankments and cuts by Argyroudis and Kaynia (2015). These states are described in terms of induced permanent ground displacement (PGD) of the slope. In view of the ensuing discussion, the limit states adopted for the study are presented in Table 7.

Methodology of Generation of Seismic Fragility Curves

The fragility curve is represented by two-parameter cumulative lognormal distribution and is mathematically represented by Eq. (7)

$$P_f(ds > ds_i|S) = \Phi\left[\frac{1}{\beta_{tot}}\ln\left(\frac{IM}{IM_{mi}}\right)\right] \quad (7)$$

where P_f represents the probability that a particular damage state, *ds*, is exceeded under the action of a given level of seismic intensity. The seismic intensity level is defined by intensity measure of earthquake, *IM*, which in the present study is represented by the peak ground acceleration (PGA) of the earthquake time histories. Φ denotes the cumulative probability function whereas IM_{mi} represents the median threshold value of the earthquake intensity measure which causes the damage associated with the ith state. β_{tot} represents the total variability associated with the fragility curves. From Eq. (7), it follows that the development of fragility curve is dependent on two parameters: IM_{mi} and β_{tot} .

The estimation of the seismic fragility curve depends on the evolution of damage index with increasing intensity of earthquake. To illustrate the procedure, consider Fig. 4 in which the various data points represent the results of numerical analyses in terms of parameter characterizing the performance of associated structure under different levels of seismic action. The solid line is obtained from regression analysis. Depending on the damage index of the ith damage state, the median threshold value of earthquake intensity measure IM_{mi} may be estimated.

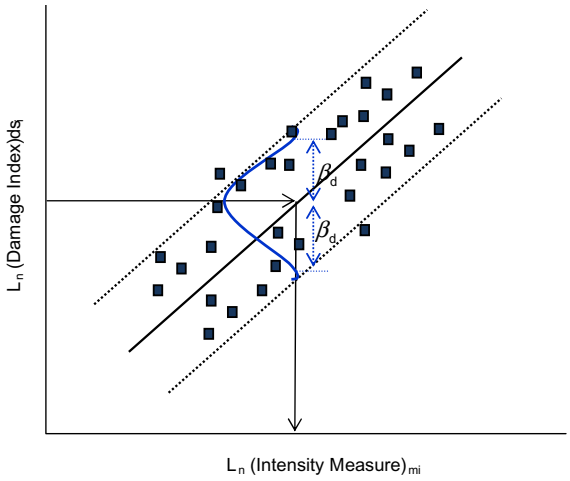

Fig. 4 Evolution of damage with earthquake intensity measure showing the standard deviation for variable input motion and the threshold median value

Since an assumption of lognormal distribution function is made for the seismic fragility curve, a lognormal standard deviation β_{tot}, describing the total variability needs to be estimated. Usually, there are three sources of uncertainty which needs to be considered (NIBS 2004). These include the definition of the damage states(β_{ds}), the response of the element or the system (β_c) and the earthquake input motion (β_D). The total variability is expressed by combination of these three contributors with the assumption that they are stochastically independent having a lognormal distribution. Thus, the lognormal standard deviation β_{tot}may be evaluated using Eq. (8). General steps of generation of seismic fragility curves are provided in flow chart shown in Fig. 5.

$$\beta_{tot} = \sqrt{\beta_{ds}^2 + \beta_c^2 + \beta_D^2} \quad (8)$$

Dynamic Analyses of the Rock Slope

For the development of the seismic fragility curve of the considered

Table 7. Definition of Damage States and Ground Displacement

Damage Index	Ground Displacement (mm)	Description
Minor	20	No effect
Slight	50	Slight cracks in roadway element
Moderate	75	Major cracks leading to slowing down of traffic
Major	100	Repair required

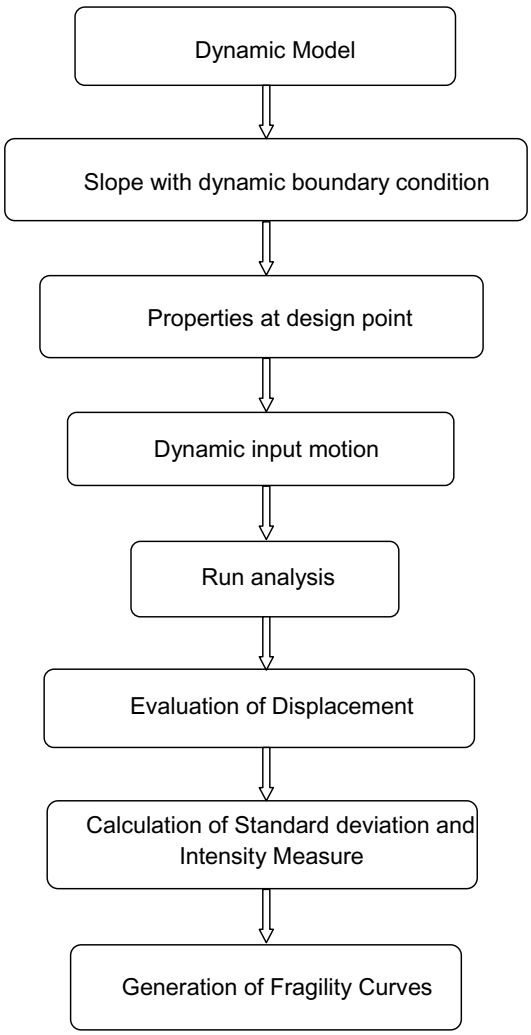

Fig.5. Flow chart showing procedure for generation of fragility curves.

slope, dynamic analyses have been carried out considering ten different earthquake time histories. Table 8 summarizes the PGA and the predominant time period of the earthquake motions considered. Each time-history has been normalized using their respective peak ground acceleration (PGA). Subsequently, all earthquake motion has been scaled in steps of 0.1g to include PGA between the ranges of 0.1g to 1.0g for numerical dynamic analyses. The 10 earthquake time histories selected for the present study encompasses the frequency range and PGA values which the slope may be subjected to during the design lifecycle. A typical acceleration time-history of Kobe earthquake (1995) considered for the dynamic analyses is shown in Fig. 6.

In the dynamic analyses, transmitting and absorbing boundary conditions have been invoked at the lateral and bottom boundaries

Table 8. Earthquake time histories considered in the study

Earthquake Name	Year	PGA (g)	Pred. Time Period (s)
Chi Chi	1999	0.18	0.80
Coyote	1979	0.12	2.40
Imperial Valley	1940	0.17	3.24
Kobe	1995	0.82	2.14
Kacaeli	1999	0.22	5.36
Loma Gilroy	1989	0.17	3.94
Loma Gilroy2	2002	0.36	3.30
Mammoth Lake	1980	0.43	2.42
Nahanni	1985	0.15	4.0
Northridge	1994	0.22	5.01

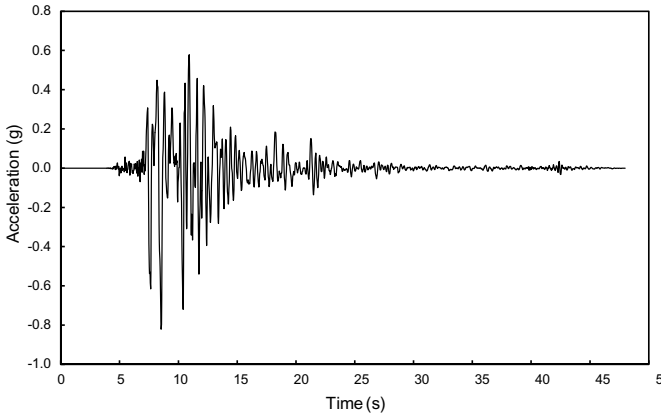

Fig.6. Acceleration time history of Kobe earthquake (1995).

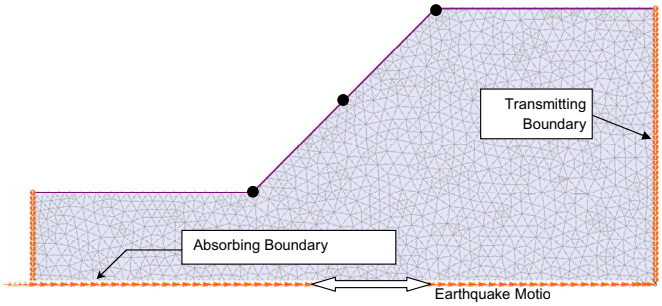

Fig.7. Boundary conditions and monitoring points for dynamic analyses of slope (monitoring points shown as black dots)

respectively to minimize the reflection of waves. For monitoring the displacements of the slope, three points along the sloping surface has been incorporated. The earthquake motion has been applied at the bottom in the horizontal direction. Fig. 7 shows the configuration of the slope model for the dynamic analyses along with the monitoring points and direction of applied dynamic motion. From these analyses, the average value of the peak displacements has been utilized for the development of fragility curves.

Derivation of Seismic Fragility Curves

The derivation of seismic fragility curves requires the definition of the median threshold value of PGA corresponding to each damage state and the total standard deviation. Based on the results of the dynamic numerical analyses, a plot showing the evolution of damage (in terms of displacement) with increasing intensity of earthquake (PGA) is obtained. The displacement shown in Fig. 8 is the average displacement recorded at three points along the slope surface as shown in Fig. 7. A regression analysis is performed on the results to

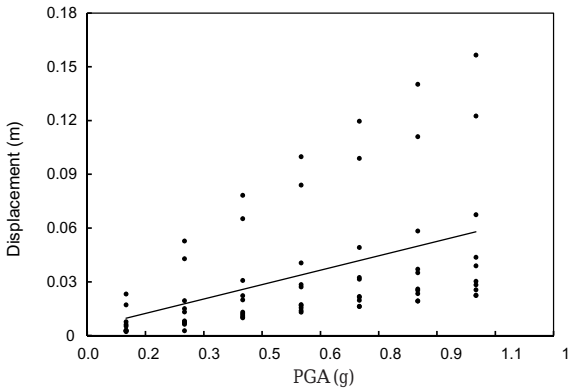

Fig.8. Evolution of damage expresses as peak displacement vs peak ground acceleration.

establish a relationship between the displacement and the intensity of the earthquake. For estimating the standard deviation, a value of 0.4 as suggested in HAZUS-MH (2004) has been adopted for β_{ds}. Moreover, the value of β_c is assigned as 0.3. The last source of uncertainty β_D is obtained from the variability in response evaluated using numerical analyses. Intensity measure is determined from the equation fitted for the displacement vs. PGA of the earthquake time histories. The intensity measures determined for each damage state considered is presented in Table 9.

Table 9. Intensity measure corresponding to each damage state

Damage State (mm)	Intensity measure
20	0.29
50	0.85
75	1.29
100	1.78

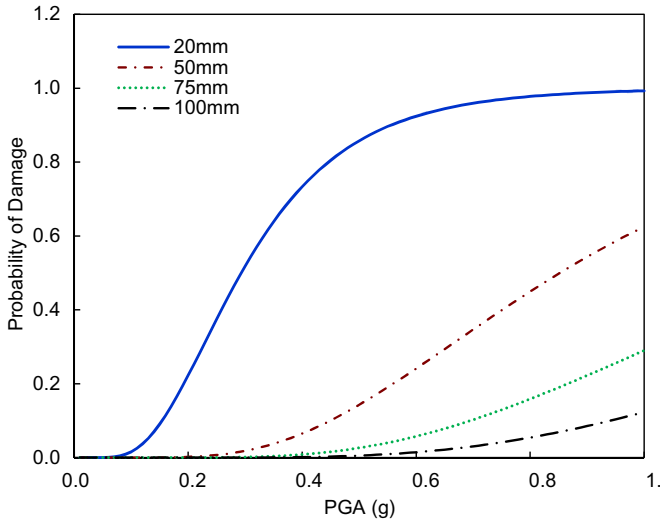

Fig.9. Final seismic fragility curves for the considered rock slope

The seismic fragility curves for the four damage states considered in the present study are shown in Fig. 9. It may be observed that the minor damages may occur at lower PGA levels. For slight damage state which is associated with crack development in roadways a PGA level greater than 0.1g is required. The probability of damage rises with an increase in PGA levels reaching a maximum of 0.6 corresponding to a PGA level of 1g. In comparison, for higher damage states i.e., moderate and severe, the probability of damage corresponding to earthquake intensity of 1.0g is 0.29 and 0.13 respectively. Moreover, these damage states do not occur at levels of shaking lower than 0.4g.

SUMMARY

Uncertainties are associated with the assessment of the seismic performance of rock slopes in the form of material variability and seismic demand. The present paper attempts to demonstrate a methodology to effectively consider both categories of uncertainty in the vulnerability assessment of a typical rock slope. Initially, pseudo-static analyses are performed to arrive at the most critical combination of variable parameters. In order to overcome the limitations of the pseudo-static analyses in effectively incorporating the variability of the seismic ground motion and the interaction of dynamic waves with the slope, dynamic analyses are performed. The earthquake time history records considered for the dynamic analyses covers a wide range of fundamental frequency and maximum amplitude. The results of the analyses are utilized in the generation of seismic fragility curve of the rock slope for various damage states. The major conclusions of the study are as following.

- For the present rock slope, slight damage state associated with crack development in roadways is probable for PGA level greater than 0.1g.
- The results suggest that the damage states which may necessitate repair works for any roadway stretch along the slope is reached at a comparatively higher level of ground shaking of 0.4g.

Hence the study suggests that the vulnerability may be estimated for the given rock slope on the basis of generated fragility curves. These may also be useful in formulating the efficient mitigation strategies and policies for pre and post-earthquake actions.

References

Andersen, K.H., Lunne, T., Kvalstad, T. and Forsberg, C.F. (2008) Deep water geotechnical engineering. Proc. of the XXIV National Conference of the Mexican Society of Soil Mechanics: Aguasclientes, 26-29 November.

Argyroudis, S. and Kaynia, A.M. (2015) Analytical seismic fragility functions for highway and railway embankments and cuts. Earthquake Engineering and Structural Dynamics, v.44 (3), pp.1863-1879.

Argyroudis, S. and Pitilakis, K. (2012) Seismic fragility curves of shallow tunnels in alluvial deposits. Soil Dynamics and Earthquake Engineering, v.35, pp.1–12.

Bucher, C.G. and Bourgund, U. (1990) A fast and efficient response-surface approach for structural reliability problems. Structural Safety, v.7 (1), pp.57–66.

Cai, F. and Ugai, K. (2000) Numerical analysis of the stability of a slope reinforced with piles. Soils Found, v.40 (1), pp.73–84.

Cavounidis, S. (1987) On the ratio of factors of safety in slope stability problems. Geotechnique, v.37 (2), pp.207–210.

Chan, C.L. and Low, B.K. (2009) Reliability analysis of laterally loaded piles involving nonlinear soil and pile behavior. Jour. Geotech. Geoenviron. Engg., v.135 (3), pp.431–43.

Cheng, Y.M., Lansivaara, T. and Wei, W.B. (2007) Two-dimensional slope stability analysis by limit equilibrium and strength reduction methods. Computers and Geotechnics, v.34(3), pp.137–150

Dawson, E.M., Roth, W.H. and Drescher, A. (1999) Slope stability analysis by strength reduction. Geotechnique, v.49(6), pp.835–840

Donald, I.B. and Giam, S.K. (1988) Application of the nodal displacement method to slope stability analysis. In: Proceedings of the 5th Australia–New Zealand conference on geomechanics, Sydney, Australia, pp.456-460

Griffiths, D.V. and Lane, P.A. (1999) Slope stability analysis by finite elements. Geotechnique, v.49 (3), pp.387–403.

Griffiths, D.V., Lin, H. and Cao, P. (2010) A comparison of numerical algorithms in the analysis of pile reinforced slopes. Proc GeoFlorida 2010 Conf, West Palm Beach, Florida 1:175–183

Hasofer, A.M. and Lind, N.C. (1974) Exact and invariant second moment code format. Jour. Engg. Mech. Div, v.100 (1), pp.111–121.

HAZUS-MH (2004) User's Manual and Technical Manuals. National Institute of Building Sciences. report prepared for the Federal Emergency Management Agency, Washington D.C., USA.

Hoek, E. (1970) Estimating the stability of excavated slopes in open cast mines. Inst. Min. and Met., Trans., v.79, pp.109A–132A.

Hoek, E. and Bray, J.W. (1977) Rock Slope Engineering. Revised Second Edition, Inst. of Min. and Met., London, 402.

Kaynia, M.A., Argyroudis, S., Mayoral, J.M., Johansson, J., Pitilakis, K. and Anastasiadis, A. (2011) Systemic Seismic Vulnerability and Risk Analysis for Buildings, Lifeline Networks and Infrastructures Safety Gain. Report for the European Project SYNER-G: (FP7-ENV- 2009-1-244061).

Li, H.Z. and Low, B.K. (2010) Reliability analysis of circular tunnel under hydrostatic stress field. Computers and Geotechnics, v.37 (1–2), pp.50–58.

Low, B.K. and Einstein, H.H. (2013) Reliability analysis of roof wedges and rockbolt forces in tunnels. Tunnelling and Underground Space Technology, v.38, pp.1–10.

Lu, Q. and Low, B.K. (2011) Probabilistic analysis of underground rock excavations using response surface method and SORM. Computers and Geotechnics, v.38 (8), pp.1008–21.

Low, B.K. and Tang, W.H. (1997) Reliability analysis of reinforced embankments on soft ground. Canadian Geotech. Jour., v.34(5), pp.672–85.

Low, B.K. and Tang, W.H. (2007) Efficient spreadsheet algorithm for first-order reliability method. Jour. Engg. Mechanics ASCE, v.133 (12), pp.1378–87.

Maruyama, Y., Yamazaki, F., Mizuno, K., Tsuchiya, Y. and Yogai, H. (2010) Fragility curves for expressway embankments based on damage datasets after recent earthquakes in Japan. Soil Dynamics and Earthquake Engg., v.30, pp.1158–67.

Matsui. T. and San, K-C. (1992) Finite element slope stability analysis by shear strength reduction technique. Soils and Foundations, v.32(1), pp.59-70.

Mollon, G., Dias, D. and Soubra, A.H. (2009) Probabilistic analysis of circular tunnels in homogeneous soil using response surface methodology. Jour. Geotech. Geoenviron. Engg., v.135(9), pp.1314–25.

Mostyn, G.R. and Li, K.S. (1993) Probabilistic slope analysis—state of play. Proceedings of Conference on Probabilistic Methods in Geotechnical Engineering. A.A Balkema, Canberra, Australia, pp.89–109.

National Institute of Building Sciences (NIBS). HAZUS-MH: Users's Manual and Technical Manuals. Report prepared for the Federal Emergency Management Agency, Washington DC, 2004.

Nilsen B (2000) New trend in rock slope stability analysis. Bull. Engg. Geol. Environ, v.58, pp.173–178.

Pathak, S and Nilsen, B. (2004) Probabilistic rock slope stability analysis for Himalayan condition. Bull. Engg. Geol. Environ, v.63, pp. 25–32.

Phoon, K.K. and Kulhawy, F.H. (1999) Characterization of geotechnical variability. Canadian Geotech. Jour., v.36(4), pp.612-624.

Pitilakis K, Crowley E, Kaynia A (Eds.) (2014) SYNER-G: typology definition and fragility functions for physical elements at seismic risk. Geotechnical, Geological and Earthquake Engineering 27p.

Rajashekhar, M.R. and Ellingwood, B.R. (1993) A new look at the response-surface approach for reliability-analysis. Structural Safety v.12(3), pp.205–20.

Rathod, G.W. and Rao, K.S. (2012) Finite element and reliability analyses for slope stability of Subansiri Lower Hydroelectric Project: a case study. Geotech. Geol. Engg., v.(30), pp.233-252.

Rocscience Inc., RS 2.0 (2015) Finite Element Analysis for Excavations and Slopes, Toronto, Canada.

Rossetto, T. and Elnashai, A. (2003) Derivation of vulnerability functions for European type RC structures based on observational data. Engineering Structures, v.25, pp.1241-1263.

Shen, Y., Gao, B., Yang, X. and Shuangjiang, T. (2014) Seismic damage mechanism and dynamic deformation characteristic analysis of mountain tunnel after Wenchuan earthquake. Engg. Geol., v.180, pp.85-98.

Song, K.I., Cho, G.C. and Lee, S.W. (2011) Effects of spatially variable weathered rock properties on tunnel behavior. Probabilistic Engineering Mechanics, v.26, pp.413-26.

Tandjiria, V., Teh, C.I. and Low, B.K. (2000) Reliability analysis of laterally loaded piles using response surface methods. Structural Safety, v.22 (4), pp.335–55.

Ugai, K. and Leshchinsky, D. (1995) Three-dimensional limit equilibrium and finite element analysis: a comparison of result. Soils and Foundatons, v.35(4), pp.1–7.

Wei, W.B., Cheng, Y.M. and Li, L.(2009) Three-dimensional slope failure analysis by the strength reduction and limit equilibrium methods. Computers and Geotechnics v.36, pp.70–80.

Wei, W.B. and Cheng, Y.M. (2009) Strength reduction analysis for slope reinforced with one row of piles. Computers and Geotechnics, v.36 (7), pp.1176–1185.

Won, J., You, K., Jeong, S., and Kim, S. (2005) Coupled effects in stability analysis of pile–slope systems. Computers and Geotechnics v.32 (4), pp.304–315.

Wyllie DC, Mah CW (2004) Rock Slope Engineering, 4th Edition, Spon Press, Taylor and Francis Group.

Xu, B. and Low, B.K. (2006) Probabilistic stability analyses of embankments based on finite element method. Jour. Geotech. Geoenviron. Engg. v.132 (11), pp.1444–54.

Yang, S., Ren, X. and Zhang, J. (2011) Study on embedded length of piles for slope reinforced with one row of piles. Jour. Rock Mech. Geotech. Engg., v.3(2), pp.167–178.

Zhang, K., Cao, P., Meng, J., Li, K. and Fan, W. (2015) Modeling the progressive failure of jointed rock slope using fracture mechanics and strength reduction method. Rock Mechanics and Rock Enginering v.48, pp.771-785.

Zienkiewicz, O.C., Humpheson, C. and Lewis, R.W. (1975) Associated and non-associated visco-plasticity and plasticity in soil mechanics. Geotechnique, v.25(4), pp.671–689.

(Received: 23 June 2017; Revised form accepted: 6 February 2018)